ELSEVIER

Environmental Modelling & Software 17 (2002) 169–178

Environmental Modelling & Software

www.elsevier.com/locate/envsoft

An optimised method to couple meteorological and photochemical models

A. Martilli [a,*], P. Thunis [b], F. Müller [c,1], A.G. Russell [d], A. Clappier [a]

[a] *Swiss Federal Institute of Technology (EPFL), Laboratoire de Pollution de l'Air et des Sols, CH-1015 Lausanne, Switzerland*
[b] *Joint Research Centre (JRC), Environment Institute, I-21020 Ispra, Italy*
[c] *University of Hamburg, Meteorological Institute, D-0146 Hamburg, Germany*
[d] *Civil and Environmental Engineering, Georgia Institute of Technology, Atlanta, GA 30332-0512, USA*

Received 12 October 2000; accepted 27 April 2001

Abstract

Accuracy of photochemical air quality model results depends not only on the accuracy of the meteorological fields supplied to the model, but also the frequency that those fields are updated. Tests in two and three dimension, with and without chemistry, were run to identify errors that can arise due to the frequency that models are linked (or coupled) to time varying meteorological fields. In applications using photochemical models uncoupled from meteorological models, the typical frequency that fields are updated is 1 h. This may lead to some error. When run in a coupled fashion, advecting trace contaminants using the same time step as the meteorological model requires excessive computational time, and does not improve results significantly beyond that found when using the CFL limit to determine the chemical species advection step.

Keywords: Air pollution; Photochemical models; Mesoscale meteorological models; Coupling techniques

Software availability

Name of the software: TVM (Topographic Vorticity Mesoscale) Model.
Brief description: TVM is a vorticity-mode, non-hydrostatic, incompressible mesoscale meteorological model coupled with a transport photochemical module.
Author's/contact: Alberto Martilli, LPAS, IGE_DGR, EPFL, CH1015, Lausanne, Switzerland.
E-mail: alberto.martilli@epfl.ch
Hardware requirements: Any workstation or PC
Software requirements: FORTRAN-77

1. Introduction

Numerical study of air quality with photochemical models requires meteorological data (at various scales). These meteorological data result from observations which are extrapolated over the whole domain to obtain mass-consistent wind fields (e.g. Goodin et al., 1980) or through prognostic models (e.g. Pielke, 1984). The latter may include meteorological data or links with observations through nudging techniques (Stauffer et al. 1990, 1991). Whatever the method, a wind-flow field is required for photochemical model calculations and the final results will crucially depend on the quality of this data. Since observations are generally available only at discrete times (e.g. hourly), diagnostic wind-fields (based on observations) are updates at those particular times. This approach is limiting since it does not incorporate the effect of atmospheric motions having smaller time-scale variations than the update time interval. This constraint is removed for prognostic meteorological models but if the two models (meteorological and photochemical) are run independently (i.e. first meteorology and afterwards photochemistry), a higher updating frequency can be problematic because all the meteorological information must be stored. On the other hand, if the two models are run simultaneously, the CPU time increases for a single simulation. Since air quality modelling studies generally require testing of several differ-

* Corresponding author. Fax: +41-21-693-5145.
E-mail address: alberto.martilli@epfl.ch (A. Martilli).
[1] Present address: Max-Planck-Institute for Meteorology, D-20146, Hamburg, Germany

1364-8152/02/$ - see front matter
PII: S1364-8152(01)00062-7

ent emission scenario, the need of re-running the meteorological model for each of these scenario may increase total CPU time. This explains why most of the existing models use relatively large updating time increments; (e.g. Chang et al., 1987), except for a few authors who applied a direct simultaneous coupling (Vogel et al., 1995; Svensson, 1995).

In this paper, a quantitative analysis of the error generated in air quality modelling by different meteorology update frequencies is carried out for the special case of a sea breeze over complex terrain. Different tests are performed, first of all in two dimensions with an idealised topography, then, in three dimensions using a real photo-smog episode over Athens (Clappier et al., 2000). Errors are quantified for both passive and reactive species. The two methods of coupling described above, i.e. coupled (run simultaneously) or decoupled (discrete update time) are discussed and a compromise which combines the advantages of low CPU and storage costs is developed and compared to the two others.

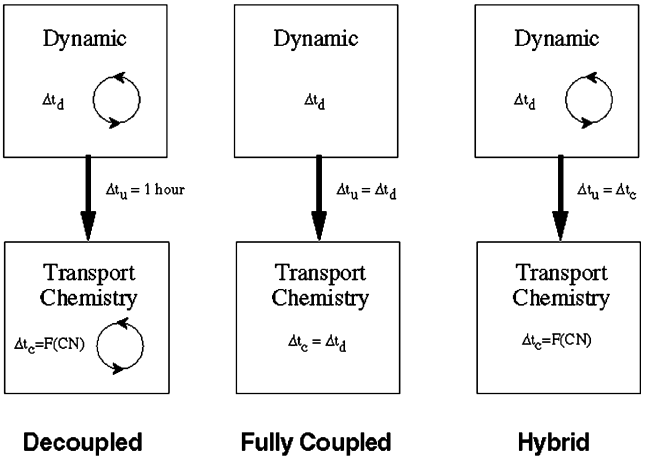

Fig. 1. Schematic representation of the three coupling techniques: decoupled, fully coupled and hybrid. Δt_d is the time step of the meteorological module (resolution of the dynamic), Δt_c is the time step of the photochemical module (resolution of the transport and the chemistry), Δt_u is the time step of the meteorology updates.

2. Models description and coupling methodologies

The impact of meteorology update time increment on air quality results is investigated here by use of the TVM (Thermal Vorticity Mesoscale) model. This model is composed of two distinct modules:

- The meteorological module is nonhydrostatic (Schayes et al., 1996; Thunis, 1995) and predicts temperature, humidity, wind fields, and turbulence.
- The photochemical module is based on that used in the CIT model (Harley et al., 1993) and solves transport, diffusion and chemical transformations for the species. The chemical mechanism is the LCC (Lurmann et al., 1987); it includes 35 species involved in 106 reactions. In this module an operator splitting is applied in the following order: (1) the transport of the pollutants is computed for half of the module time step, (2) the chemistry and the turbulent diffusion are solved simultaneously for the module time step and (3) the transport is computed for half of the module time step. This technique permits to alternate the order of resolution of the transport and chemistry/diffusion and it avoids possible errors induced by an arbitrary choice of the order of resolution.

The photochemical modules require information from the meteorological module such as wind field for mean transport, diffusion coefficients for turbulent transport and temperature for rate coefficients. The accuracy of the results depends on the frequency with which meteorology updates are made. In this work, three different methodologies are compared (Fig. 1):

1. *Decoupled*: The meteorological and photochemical modules are run independently. Meteorology is run first with an internal time step (Δt_d) that is determined by the interactions between thermodynamic and dynamic fields. Generally, it ranges from 5 to 30 s. Meteorology is updated into the photochemical module on an hourly basis (Δt_u=1 h). The photochemical module operates with an internal time step (Δt_c) defined as follows: Δt_c=CN/max($U/\Delta x$, $V/\Delta y$, $W/\Delta z$) with CN being the Courant number; U, V and W the three wind components; and, Δx, Δy, Δz the cells sizes in the three directions. If the Courant number (CN) exceeds 1 (Courant Friedrich Levy condition), the distance travelled in one time step due to the transport is greater than the grid separation and instabilities occur. In the cases considered here, when CN=1, the resulting time step ranges from 100 to 1000 s depending on the wind field intensity. We also made some test using other limits to the advection time steps, e.g. CN=0.1 and 0.5. Note that most air quality models currently follow this decoupled methodology.
2. *Full coupling*: The photochemical module is placed on-line with the meteorology. At every time step the meteorological module and the photochemical module (using the updated meteorological variables) are solved using the same time step. The latter is then fixed as the minimum of the two previously discussed internal time steps (Δt_d and Δt_c). This methodology provides the most accurate results since photochemistry is always calculated using the most recent meteorological data; it will therefore serve as reference in the discussion hereafter.
3. *Hybrid coupling*: Meteorology is updated when Δt_c used in the photochemical model is reached.

3. Two dimensional tests

3.1. Description of the meteorology

An idealised 2D case consisting of a Gaussian shape mountain (height: 500 m, half width: 10 km) bounded on its left side by a 25 km wide water surface is studied here. The modelling domain is 80 km long by 8 km high and is divided into 57 horizontal by 11 vertical grids. In the horizontal direction the finest resolution is 1km in the central part of the domain and the grid is horizontally stretched at the two borders. In the vertical direction the grid is stretched up the model top. Simulations start at 06:00 LST and last for 24 h. Fig. 2 shows the flow-field pattern at 12:00 [Fig. 2(a)], 17:00 [Fig. 2(b)] and 20:00

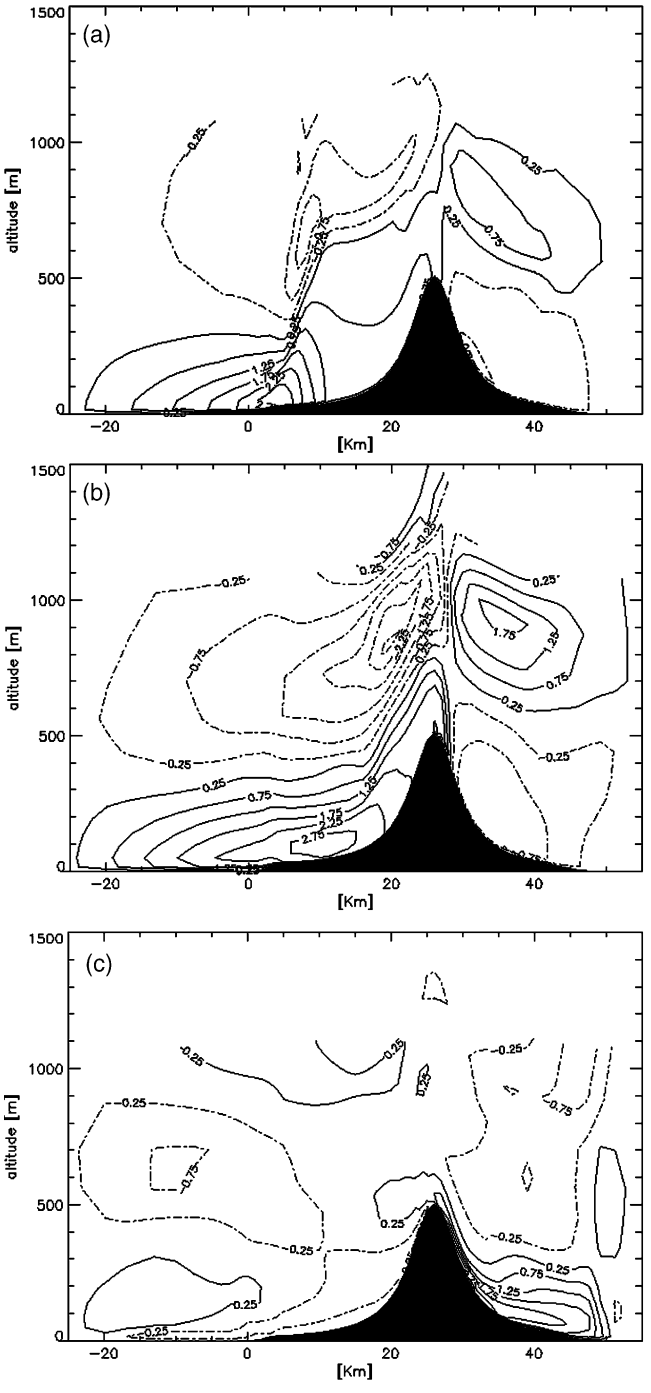

Fig. 2. Vertical cross sections of the east–west wind field at different times: (a) at 12:00 LST, (b) at 17:00 LST, (c) at 20:00 LST. Solid and dotted lines are for positive and negative values, respectively. Values located on the left of abscissa 0 are over the sea.

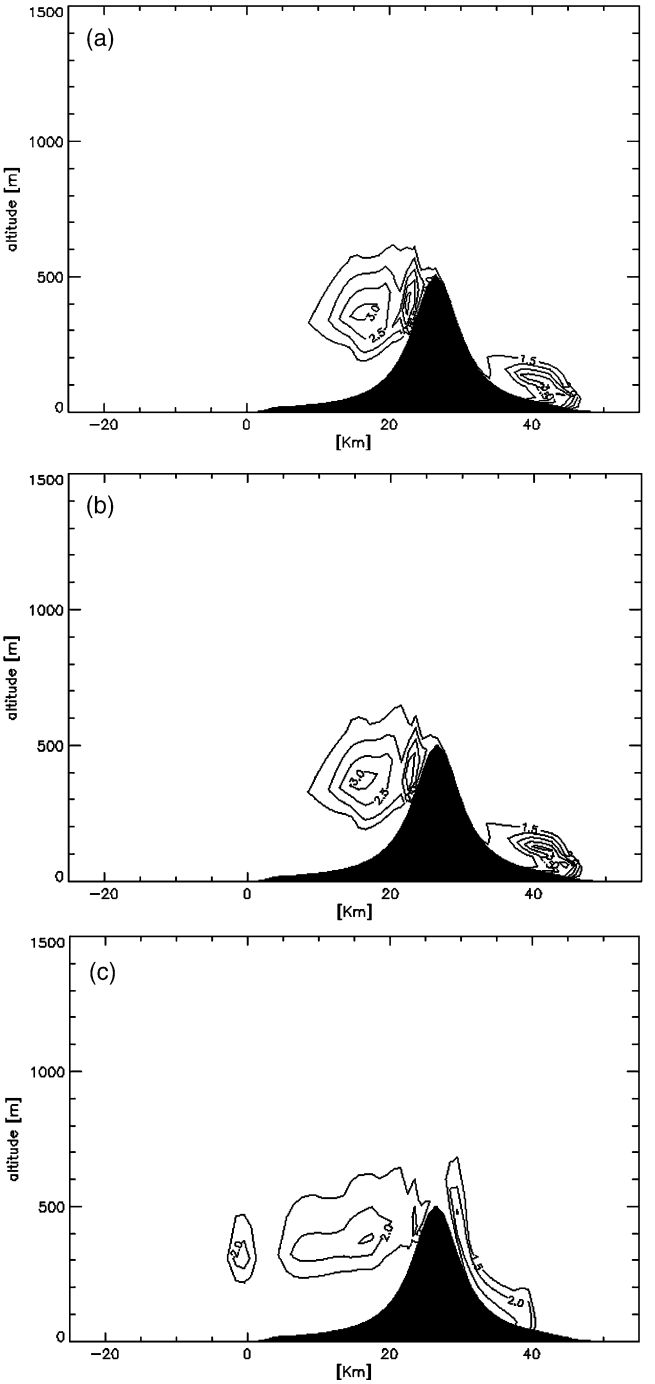

Fig. 3. Puff position for the passive tracer 5 h after release for the different coupling methods: (a) full coupling; (b) hybrid (CN=1) (c) decoupled (CN=1).

Table 1
Maximum (left column) and mean (right column) differences for the passive tracer test for different techniques and Courant number. Values are in percent

Passive tracer	CN=0.1		CN=0.5		CN=1.0	
	Max.	RMS diff.[a]	Max.	RMS diff.	Max.	RMS diff.
Hybrid	0.4	0.0	7.3	0.9	14.7	1.9
Decoupled	88.5	15.1	88.5	15.2	88.5	15.3

[a] Root mean square difference

LST [Fig. 2(c)], with the typical features expected from differential heating: land/sea breeze and anabatic–katabatic winds on both sides of the mountain. This complex flow field, which evolves rapidly with time, is well suited to study the impact of updating frequency on air quality modelling results. This impact is quantified using, first, a passive tracer and, second, the reactive gas phases species of LCC.

3.2. Passive tracer

In this case, a passive tracer puff (a dimensionless concentration of 100 located at 2 km from the coast inland, 150 m above the surface) is emitted at 15:00. The background concentration is set to 1. Results for the three coupling methods at 20:00 LST are represented in Fig. 3. For each method, the passive tracer concentration is divided in two puffs at the right and left side of the mountain. The hybrid results [Fig. 3(b)] are very similar to those obtained with the full coupling method [Fig. 3(a)] while some differences in the spatial repartition and the maximum of both puffs are observed in the case of the decoupled technique [Fig. 3(c)]. For the hybrid method and especially for the decoupled method the results (not shown) obtained with an updating frequency corresponding to CN=0.1 and 0.5 are very similar to the results obtained with CN=1 (see maximum differences in Table 1).

In Table 1, the maximum and mean differences between the fully and other coupling methodologies is

Table 2
Maximum (Left column) and mean (right column) differences for O_3, NO_x, VOC and HO_2 for the reactive tracer rest for different techniques and different Courant number. Values are in percent

O_3 at 17:00 LST	CN=0.1		CN=0.5		CN=1.0	
	Max.	RMS diff.[a]	Max.	RMS diff.	Max.	RMS diff.
Hybrid	0.2	0.0	1.9	0.2	5.3	0.5
Decoupled	51.9	8.7	51.7	8.7	51.2	8.6
NO_x at 17:00 LST						
Hybrid	0.7	0.0	4.6	0.3	12.3	0.9
Decoupled	37.7	4.6	37.5	4.6	35.4	4.5
VOC at 17:00 LST						
Hybrid	1.1	0.1	5.7	0.3	12.8	1.0
Decoupled	41.0	4.5	40.4	4.5	38.6	4.4
HO_2 at 17:00 LST						
Hybrid	1.3	0.2	4.3	1.5	27.1	5.2
Decoupled	54.1	9.1	54.6	9.1	55.6	9.3

[a] Root mean square difference

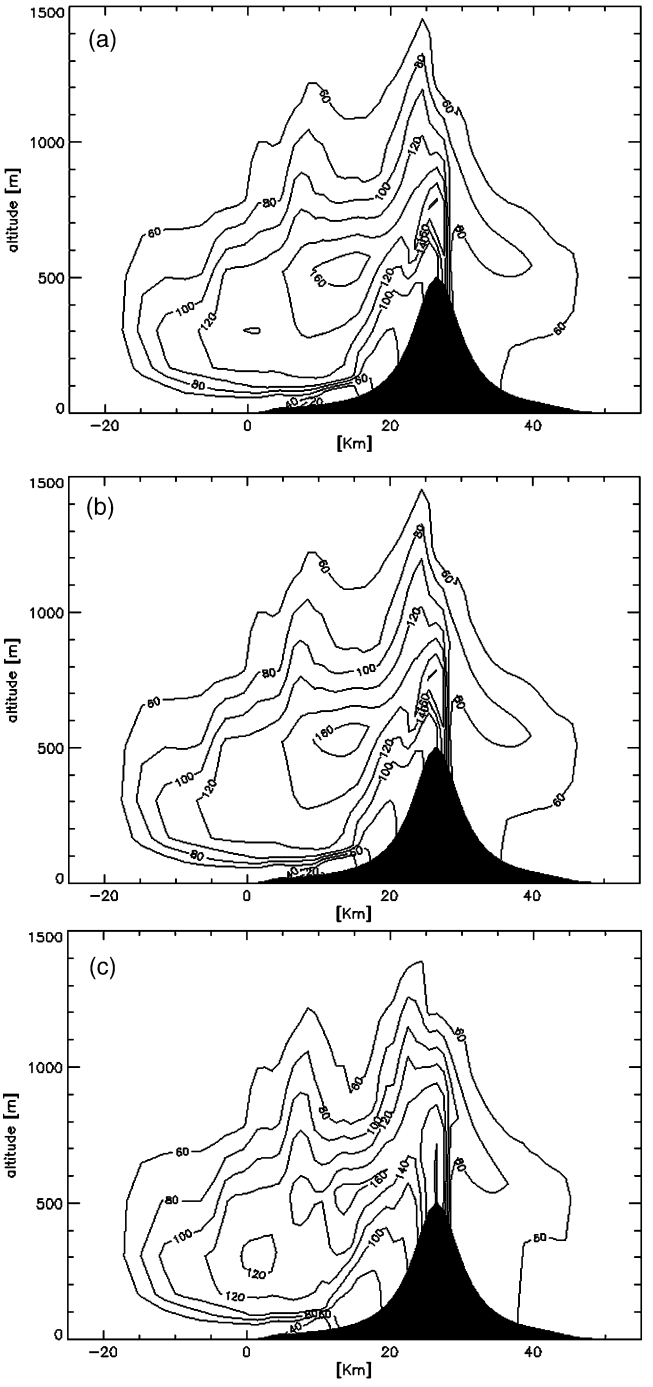

Fig. 4. O_3 concentration in ppm at 17:00 LST for the different coupling methods: (a) full coupling; (b) hybrid (CN=1); (c) decoupled (CN=1).

given using the following definitions: the normalised difference 'diff', is computed via:

$$\mathrm{diff}_{ij} = 100 \cdot \left| \frac{c_{ij} - c'_{ij}}{c_{\max}} \right| \quad (1)$$

where

c_{ij} is the concentration at the grid point ij for the hybrid and the decoupled cases,

c'_{ij} is the concentration for the fully coupled case, $c_{\max} = \max_{\substack{i=1,nx \\ j=1,nz}} (|c_{ij} - cb|, |c'_{ij} - cb|)$

c_b is the background value and nx and nz the number of points in the horizontal and the vertical direction respectively.

The maximum normalised difference is

$$\mathrm{diff}_{\max} = \max_{\substack{i=1,nx \\ j=1,nz}} (\mathrm{diff}_{ij}) \quad (2)$$

The root mean square normalised difference is computed by mean of the normalised difference Eq. (1):

$$\mathrm{rmsdiff} = \sqrt{\frac{1}{nx \cdot nz} \sum_{\substack{i=1,nx \\ j=1,nz}} (\mathrm{diff}_{ij})^2} \quad (3)$$

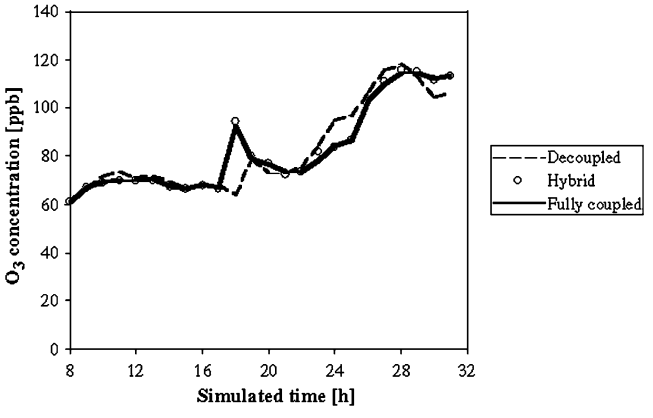

Fig. 5. Time evolution of O_3 concentration (in ppb) near the ground (30 m) at a specific location (30 km inland on the mountain slope opposite to the emission source) for the different coupling techniques.

Table 1 shows that difference between the decoupled (with hourly interval) and the full coupled method (RMS of 15.3 for CN=1) is much larger than the difference between the hybrid and fully coupled method (RMS of 1.9). It is interesting to note that this RMS error increases with the size of the time step for the hybrid method while it is not the case for the decoupled one. Indeed, in the latter case, most of the error is due to the poor frequency of meteorology updates and the numerical error generated by the different Courant number only slightly modulates this error. On the contrary, in the case of the hybrid method, most of the error is now only due to the numeric since the meteorology update frequency is relatively high.

3.3. Reactive tracer

In this case, a source is located between the shoreline and the mountain. It emits volatile organic compounds

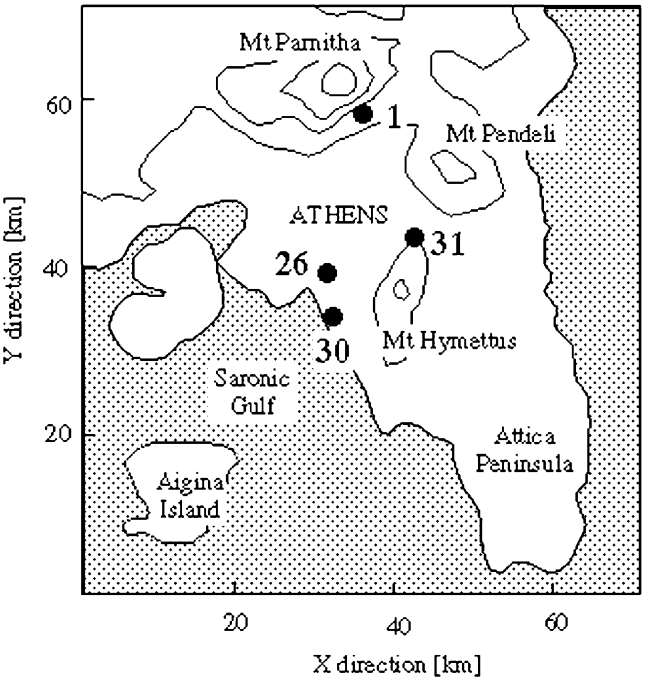

Fig. 7. Map of the Greater Athens area.

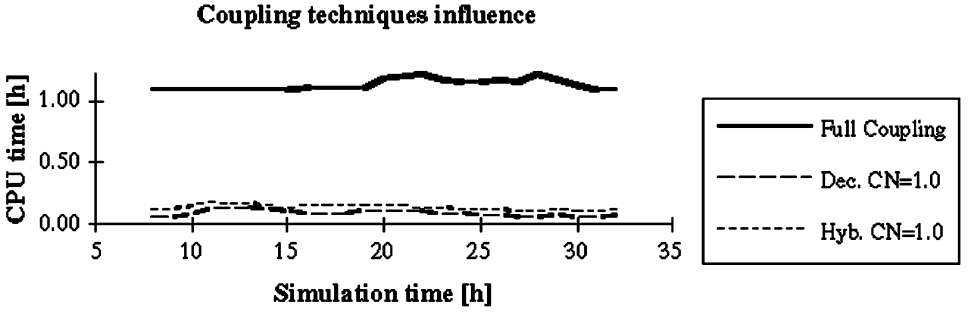

Fig. 6. Required simulation time for the different coupling techniques.

(VOC), nitrogen oxides (NO_x) and CO at a rate typical of an urban area. The evolution of both primary and secondary (e.g. ozone) species is here followed. Simulations start at 08:00 LST, Fig. 4 shows the resulting O_3 concentrations after 9 h of simulation (at 17:00 LST). The maximum difference between the decoupled and fully coupled method reaches 51.2% for ozone and 35.4% for NO_x (Table 2) while they are drastically reduced to 5.3% and 12.3% respectively, for the hybrid method. These maximum differences are all observed in the vicinity of the surface where wind time variations are the more dramatic. The RMS differences illustrate the same trend, i.e. evolving from 8.6% (O_3) and 4.5% (NO_x) for the decoupled results to 0.5 and 0.9% for the hybrid one.

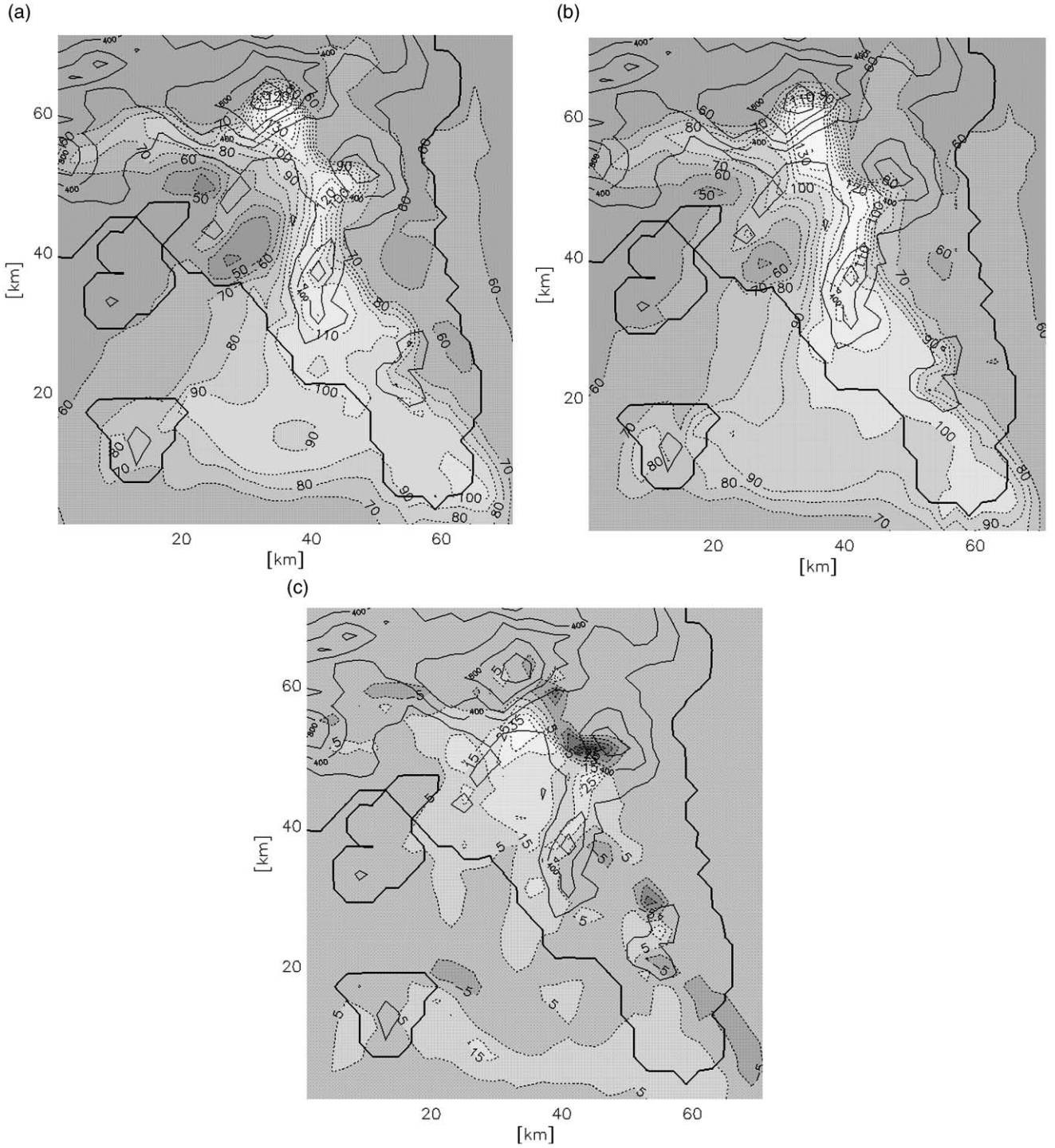

Fig. 8. Simulated distribution near the ground (30 m deep) at 17:00 LST: (a) O_3 concentration (in ppb) obtained with the hybrid method; (b) O_3 concentration (in ppb) obtained with the decoupled method; (c) difference (in ppb) between the decoupled and the hybrid methods.

Results for the VOC concentrations are almost similar to those obtained for NO_x. For a highly reactive species, like HO_2, the differences between the decoupled and the fully coupled techniques are of the same order of that of O_3 (e.g. 55.6% for the peak and 9.3% for the RMS, Table 2). With the hybrid method the differences are smaller (27.1% for the peak and 5.2 for the RMS), but the reduction is less strong than that for O_3.

The impact of coupling methodologies therefore becomes important for complex terrain areas in which rapidly evolving winds are observed.

For both reactive and passive tracers, important differences, which appear where pollutant gradients are large, are then advected throughout the domain. This means that if one looks at the predicted temporal evolution of a pollutant at one location, the greatest differences occur only during a relatively short time period while afterwards, the different methods give similar results (Fig. 5). This does not mean that the error suddenly dissipated; it was instead advected to another downwind location.

While the hybrid and fully coupled methods produce quite similar results, the CPU time required by the decoupled and hybrid methods (Fig. 6) are approximately an order of magnitude smaller than that required by the fully coupled method (all test cases were run on a SUN SPARC 10). This dramatic decrease in CPU requirement between the hybrid and fully coupled method arises from the way the chemical solver typically works.

The chemical solver (Young and Boris, 1977) uses very short time steps at the beginning of a calculation (the time step then increases as calculation proceeds), and this is repeated after each transport step. This creates then a major CPU penalty whenever chemical integration has to be repeated frequently (e.g. McRae et al., 1982). This CPU penalty can even be larger for other methods, e.g. Gear-type solvers like LSODE (Hindmarsh, 1974) or SMVGEAR (Jacobson and Turco, 1995). On the other hand, a QSSA (Hessdvelt et al., 1978) solver would not lead to this kind of problem since their constant time step through the whole calculation does not enable them to take advantage of larger transport time steps.

The choice of the transport time step alters both CPU requirements and model accuracy. As already discussed in the passive tracer section, the use of different transport time step (0.1, 0.5 and 1 for CN) was shown to lead only to slight changes in model accuracy (Table 2) but the CPU required for these three simulations is significantly modified. Indeed, the CN=0.1 case requires approximately ten times more CPU than the two other cases (CN=0.5 and CN=1). The hybrid method is therefore time efficient only for large time steps.

4. Three-dimensional tests

For the purpose of testing in three-dimensional applications the different coupling methodologies presented earlier, the region of Athens is used. The complex atmospheric circulation induced by the hilly topography

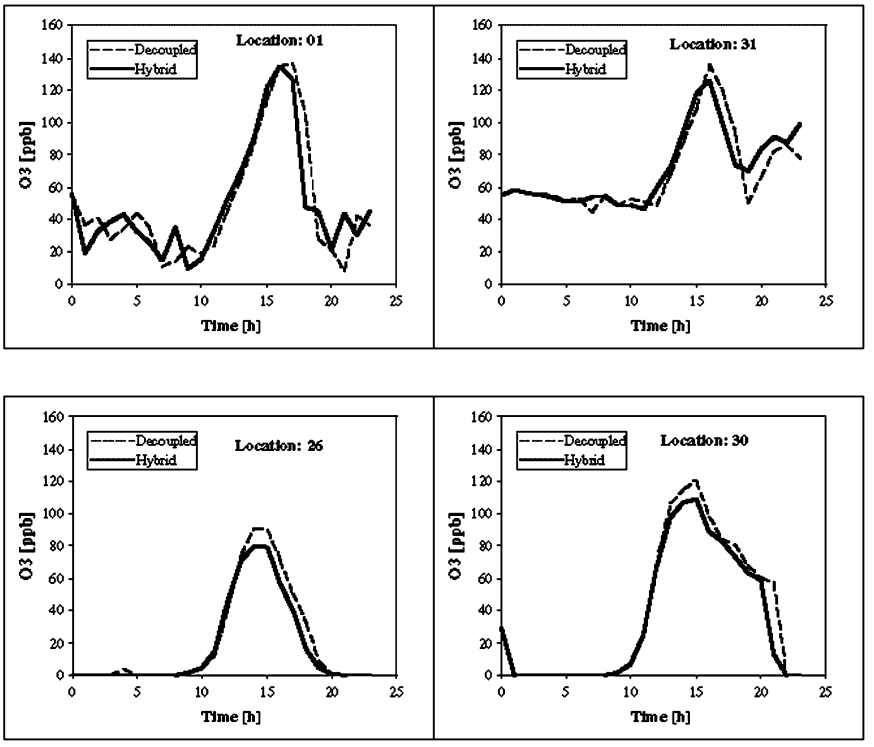

Fig. 9. O_3 time evolution at different location for the hybrid and decoupled method. The different locations are shown in Fig. 7.

and the presence of the sea on two sides (Fig. 7) makes it a very interesting area to study. Temporal wind variations associated with both slope and sea breeze are expected to occur within relatively short time periods and results could therefore be affected by the choice of the meteorology-updating interval.

In previous works, Clappier et al. (2000) and Grossi et al. (2000) presented a study of the meteorological circulation in this area as well as their implications on photochemistry using the modelling system TVM. The simulations carried out in the frame of those works will be used to test the impact of the coupling techniques. Note that due to computer requirements, the fully coupled methodology will not be considered in the case of 3-D applications.

The comparison of the hybrid and de-coupled (1 h interval) results for O_3 leads to the following comments:

1. The absolute maximums reached in the domain over a 24 h cycle are similar for both methods (145 ppb at 16:00 LST for de-coupled, 144 ppb at 17:00 LST for hybrid) but do not occur at the same time, the hybrid peak occurring 1 h prior to the de-coupled one.
2. Fig. 8(c) represents the map of differences between the decoupled and the hybrid methods for O_3 near the ground (30 m) at 17:00 LST. It shows negative values located on the NE edge of the O_3 cloud and a larger extension of positive values over the city, on the SW side of the cloud. From this comparison it is possible to deduce that the decoupled method (1) underestimates the O_3 peak (140 ppb instead of 144 ppb for the hybrid method), (2) shifts slightly ($\approx$2 km) this peak to the SW, and (3) overestimates the horizontal extension of the high concentration O_3 cloud.
3. From the time behavior at different stations (Fig. 9), one can see that the previous comments still hold. The maximum O_3 values are general coupled method. Large differences between the two methods only occur at very particular times due to the time-shift between the two coupling methods.

From the same figure, we also see that the de-coupled peak occurs over a longer time period (more spread over time), which implies that the time integral of O_3 values differ for the two methods. This can be illustrated by considering the AOT (Accumulated Exposure over a Threshold value) values. The comparison of AOT 60, i.e. the accumulated exposure over 60 ppb (used as a reference value for human health considerations), for de-coupled and hybrid methodologies (Fig. 10) indicates that differences are large and spread over the whole domain. The maximum normalised difference (Table 3) over the whole domain is found to be on the order of 25% and is therefore far from being negligible in policy-making applications. The same comparison for AOT 40 leads to a mean domain difference of about 17%, indicating that the overestimation arising from de-coupling mainly affects the high ozone concentrations. This numerical inaccuracy may contribute to poorer model performance, though is likely a small component of total model error.

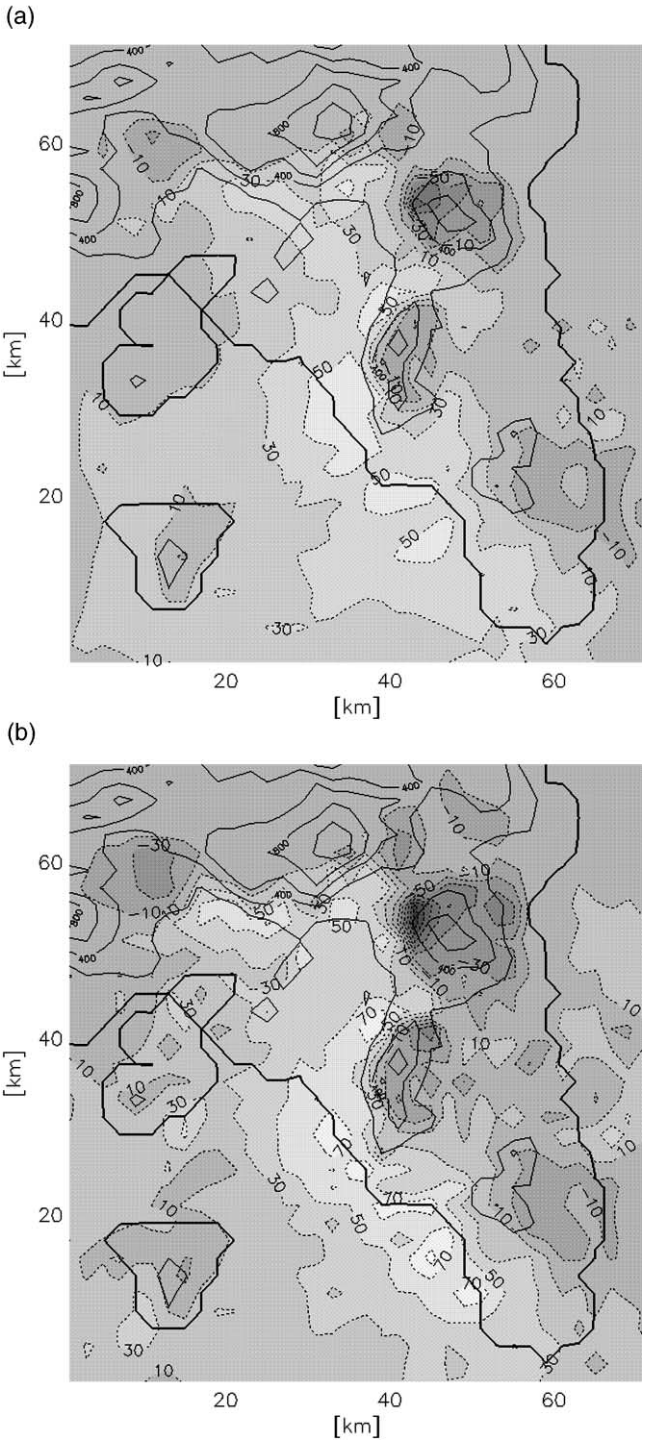

Fig. 10. Simulated distribution near the ground of the difference between the AOT (in ppb.h) computed with the decoupled and the hybrid methods: (a) AOT 60; (b) AOT 40.

For what concerns NO_x predictions (Fig. 11), the time

Table 3
Maximum (left column) and mean (right column) differences between the decoupled and the hybrid methods for O_3, AOT 60 and AOT 40 for the simulation over Athens. Values are in percent

O_3 at 17:00 LST		AOT 60		AOT 40	
Max.	RMS diff.[a]	Max.	RMS diff	Max.	RMS diff
59.4	8.9	25.1	5.3	17.0	3.5

[a] Root mean square difference

evolution at two different stations shows that the decoupled method leads to significant differences with the hybrid one. In the case of primary pollutants, this can be explained by the rough update frequency of turbulence that will over or underestimate the height over which mixing occurs.

5. Conclusions

Air quality numerical studies require the coupling of meteorological data to photochemical models. Most of the time, this coupling is realised in a non-simultaneous way, i.e. first meteorology and then chemistry. This study has shown that significant errors may be generated in gas-phase photochemical modelling if meteorological field update intervals are too coarse to resolve wind-field time variations. It was demonstrated that the so-called hybrid method in which meteorology updates are made each few minutes (Courant Friedrich Levy condition) was a good compromise between the full coupled (updates each 20 s) and decoupled (hourly updates) methods. Indeed this method proved to keep a level of accuracy very close to full coupling while CPU time was kept similar to the decoupled method. The hybrid method may also work in a decoupled way but storage of the meteorological data is large. Note the main disadvantage of the hybrid method lies in the fact that, for each tested emission scenario, meteorology must be calculated again. But it seems to be an acceptable price to correctly simulate the effect of rapidly changing windfields.

The impact of different transport time steps in the photochemical model is investigated. Concentrations resulting of three different time steps calculations were compared and it showed that smaller transport time steps improve results for the hybrid method but only slightly for the decoupled method. Most part of the error was due not to the loss of accuracy of the numerical advection scheme for longer time steps but to the updating frequency. Results obtained with a time step equal to the CN, although they were the worse of the three results, were still very similar to the reference fully coupled results. This hybrid method is therefore, a good compromise between the fully coupled and decoupled method. These results also suggest that fully coupled meteorological and air quality models could be accurate but would not use computational resources efficiently.

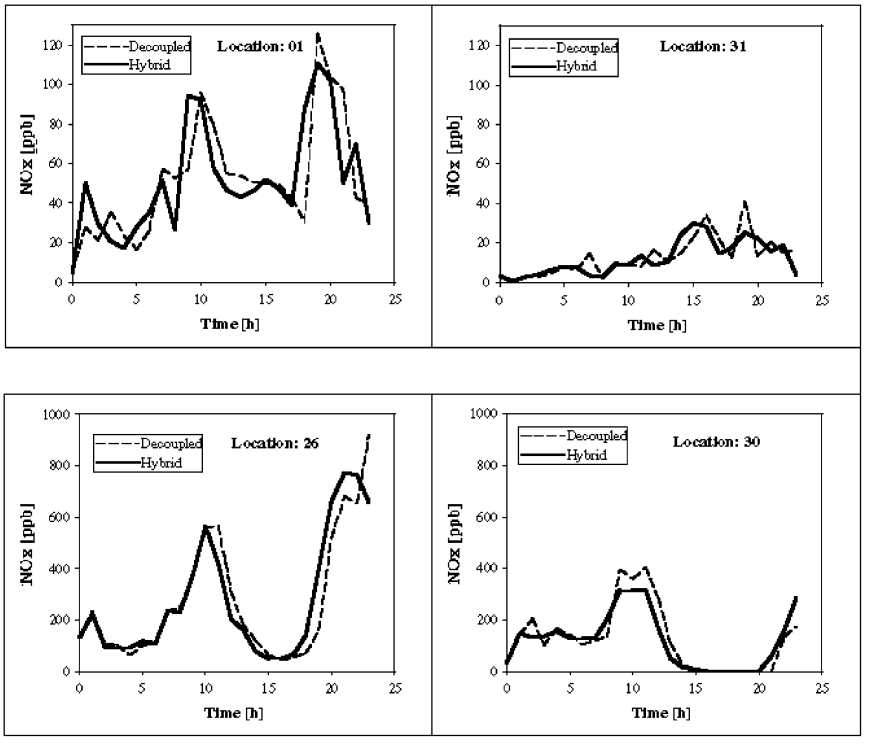

Fig. 11. NO_x time evolution at different location for the hybrid and decoupled method. The different locations are shown in Fig. 7.

References

Chang, J.S., Brost, R.A., Isaksen, I.S.A., Madronich, S., Middelton, P., Stockwell, W.R., Walcek, C.J., 1987. A three dimensional Eulerian acid deposition model: physical concepts and formation. J. Geophys. Res. 92, 14681–14700.

Clappier, A., Martilli, A., Grossi, P., Thunis, P., Pasi, F., Krueger, B.C. et al., 2000. Effect of sea breeze on air pollution in the Greater Athens area. Part I: numerical simulations and field observations. J. Appl. Meteor. 39, 546–562.

Goodin, W.R., McRae, G.J., Seinfeld, J.H., 1980. An objective analysis technique for constructing three-dimensional urban-scale wind fields. J. Appl. Meteor. 19, 98–108.

Grossi, P., Thunis, P., Martilli, A., Clappier, A., 2000. Effect of sea breeze on air pollution in the Greater Athens area. Part II: analysis of different emission scenarios. J. Appl. Meteor. 39, 563–575.

Harley, R.A., Russel, A.G., McRae, G.J., Cass, G.J., Seinfeld, J.H., 1993. Photochemical air quality modelling of the Southern California Air Quality Study. Envir. Sci. Technol. 27, 378–388.

Hessdvelt, E., How, Ø., Isaken, I., 1978. A numerical method to predict secondary air pollutants with an application oxidant generation in an urban atmosphere. WHO 810, 219–226.

Hindmarsh, A.C., 1974. GEAR: ordinary differential equation system solver. Report 4CIVD-3000 1 Rev.3, Lawrence Livermore National Laboratory.

Jacobson, M.Z., Turco, R.P., 1995. SMU-GEAR A sparse-matrix, vectorized GEAR code for atmospheric models. Atmos. Envir. 17, 273–284.

Lurmann, F.W., Carter, W.P., Coiner, L.A., 1987. A surrogate species chemical reaction mechanism for urban-scale air quality simulations models, EPA report No. 600/3-87/014B

McRae, G.J., Russel, A.G., Harley, R.A., 1982. CIT Photochemical Airshed Model—Data Preparation Manual. Carnegie Mellon University, Pittsburgh, PA.

Pielke, R.A., 1984. Mesoscale Meteorological Modelling. Academic Press, New York.

Schayes, G.P., Thunis, P., Bornstein, B.D., 1996. Development of the topographic vorticity mode mesoscale (TVM) model: Part I—formulation. J. Appl. Meteor. 35 (10), 1815–1823.

Stauffer, D.R., Seaman, N.L., 1990. Use of four-dimensional data assimilation in a limited-area mesoscale model. Part I: experiments with synoptic-scale data. Mon. Wear Rev. 118, 1250–1277.

Stauffer, D.R., Seaman, N.L., Binkowsky, F.S., 1991. Use of four-dimensional data assimilation in a limited-area mesoscale model. Part II: effects of data assimilation within the planetary boundary layer. Mon. Wear Rev. 119, 734–753.

Svensson, G., 1995. Mesoscale modelling of chemical and meteorological processes in the atmosphere. PhD dissertation, Uppsala University, Sweden.

Thunis, P., 1995. Formulation and evaluation of a nonhydrostatic vorticity-mode mesoscale model. PhD dissertation, Universite Catholique de Louvain la Neuve, Belgium.

Vogel, B., Fiedler, F., Vogel, H., 1995. Influence of topography and biogenic volatile organic compounds emission in the state of Baden–Wurttemberg on ozone concentrations during episodes of high air temperatures. J Geophys. Res. 100, 22907–22928.

Young, T.R., Boris, J.P., 1977. A numerical technique for solving stiff ordinary differential equations associated with the chemical kinetics of reactive flow problems. J. Phys. Chem. 81, 2424–2427.